

# **Dynamics of spike- and nucleocapsid specific immunity during long-term follow-up and vaccination of SARS-CoV-2 convalescents**

Nina Koerber<sup>1,+</sup>, Alina Priller<sup>2,+</sup>, Sarah Yazici<sup>2,+</sup>, Tanja Bauer<sup>1,3,+</sup>, Cho-Chin Cheng<sup>1</sup>, Hrvoje Mijočević<sup>1</sup>, Hannah Wintersteller<sup>2</sup>, Samuel Jeske<sup>1</sup>, Emanuel Vogel<sup>1</sup>, Martin Feuerherd<sup>1</sup>, Kathrin Tinnefeld<sup>1</sup>, Christof Winter<sup>4</sup>, Jürgen Ruland<sup>4</sup>, Markus Gerhard<sup>5</sup>, Bernhard Haller<sup>6</sup>, Catharina Christa<sup>1</sup>, Otto Zelger<sup>7</sup>, Hedwig Roggendorf<sup>2</sup>, Martin Halle<sup>7</sup>, Johanna Erber<sup>8</sup>, Paul Lingor<sup>9</sup>, Oliver Keppler<sup>10,3</sup>, Dietmar Zehn<sup>11</sup>, Ulrike Protzer<sup>1,3,+</sup>, Percy A. Knolle<sup>2,3,+</sup>

<sup>1</sup>Institute of Virology, Helmholtz-Zentrum München/Technical University of Munich, School of Medicine; <sup>2</sup>Institute of Molecular Immunology and Experimental Oncology, Technical University of Munich, School of Medicine; <sup>3</sup>German Center for Infection Research (DZIF), Munich partner site; <sup>4</sup>Institute of Clinical Chemistry, Technical University of Munich, School of Medicine; <sup>5</sup>Institute of Medical Microbiology, Immunology and Hygiene, Technical University of Munich, School of Medicine; <sup>6</sup>Institute of Medical Informatics, Statistics and Epidemiology, Technical University of Munich, School of Medicine; <sup>7</sup>Institute of Sports Medicine, Technical University of Munich, School of Medicine; <sup>8</sup>Department of Internal Medicine II, Technical University of Munich, School of Medicine; <sup>9</sup>Department of Neurology, Technical University of Munich, School of Medicine; <sup>10</sup>Max von Pettenkofer Institute & Gene Center, Department of Virology, Ludwig-Maximilians-University Munich; <sup>11</sup>Institute of Animal Physiology and Immunology, Technical University of Munich, School of Life Sciences.

Supplementary Figures 1-9

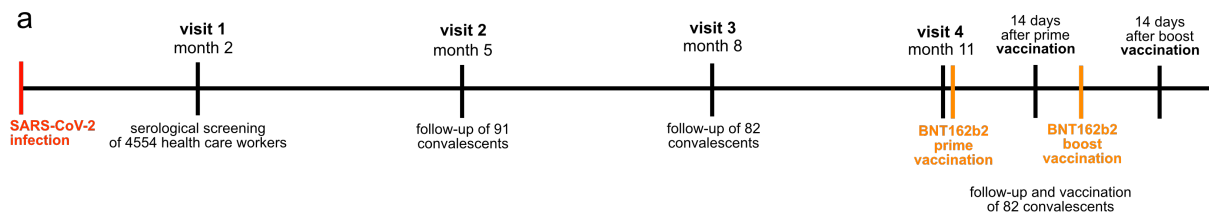
Legends to Supplementary Figures 1-9

Data availability statement

Correspondence:

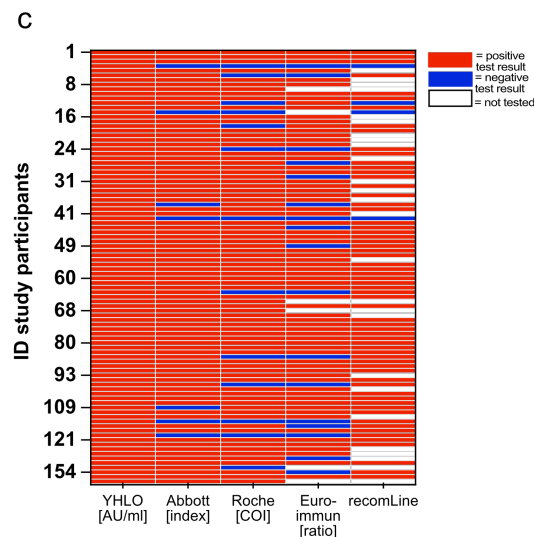
Percy A. Knolle, MD  
Institute of Molecular Immunology and Experimental Oncology  
Technical University of Munich, School of Medicine  
Ismaningerstr. 22  
81675 München  
[Percy.Knolle@tum.de](mailto:Percy.Knolle@tum.de)

Ulrike Protzer, MD  
Institute of Virology  
Technical University of Munich, School of Medicine/Helmholtz Zentrum München  
Trogerstr. 30  
81675 München  
[protzer@tum.de](mailto:protzer@tum.de)



**b**

study visits	time point	study steps	evaluated parameters	convalescent individuals	naïve individuals
visit 1	month 2	serological screening	anti-SARS-CoV-2 IgG (CLIA, YHLO)	108	4446
		participants with written informed consent to participate in study	naïve individuals: seronegative, paired matching (age, sex, occupation, exposure to COVID-19 patients)	94	53
		confirmation of infection by complementary testing	convalescent: $\geq 2$ positive test results for anti-SARS-CoV2 detection by CLIA using assays from Roche, Abbott, Euroimmun, and immunoblots using RecombiLine, virus-neutralization activity by cell culture neutralization assay ( $IC_{50}$ )	91	53
visit 2	month 5	evaluation of SARS-CoV-2 specific immunity	anti-SARS-CoV-2 IgG, virus-neutralization activity by cell culture neutralization assay ( $IC_{50}$ ), surrogate virus-neutralization activity, (Fluorospot analysis, intracellular cytokine staining when samples available)	91 (88)	53 (52)
visit 3	month 8	evaluation of SARS-CoV-2 specific immunity	anti-SARS-CoV-2 IgG, virus-neutralization activity by cell culture neutralization assay ( $IC_{50}$ ), surrogate virus-neutralization activity	82	52
visit 4	month 11	evaluation of SARS-CoV-2 specific immunity	anti-SARS-CoV-2 IgG, virus-neutralization activity by cell culture neutralization assay ( $IC_{50}$ ), surrogate virus-neutralization activity, (Fluorospot analysis when samples available)	82 (49)	53 (39)
vaccination (vacc)	14 days after prime vaccination	evaluation of SARS-CoV-2 specific immunity	anti-SARS-CoV-2 IgG, surrogate virus-neutralization activity, (Fluorospot analysis when samples available)	82 (52)	53 (50)
boost	14 days after boost vaccination	evaluation of SARS-CoV-2 specific immunity	anti-SARS-CoV-2 IgG, surrogate virus-neutralization activity, (Fluorospot analysis, intracellular cytokine staining when samples available)	33 (23)	53 (41)

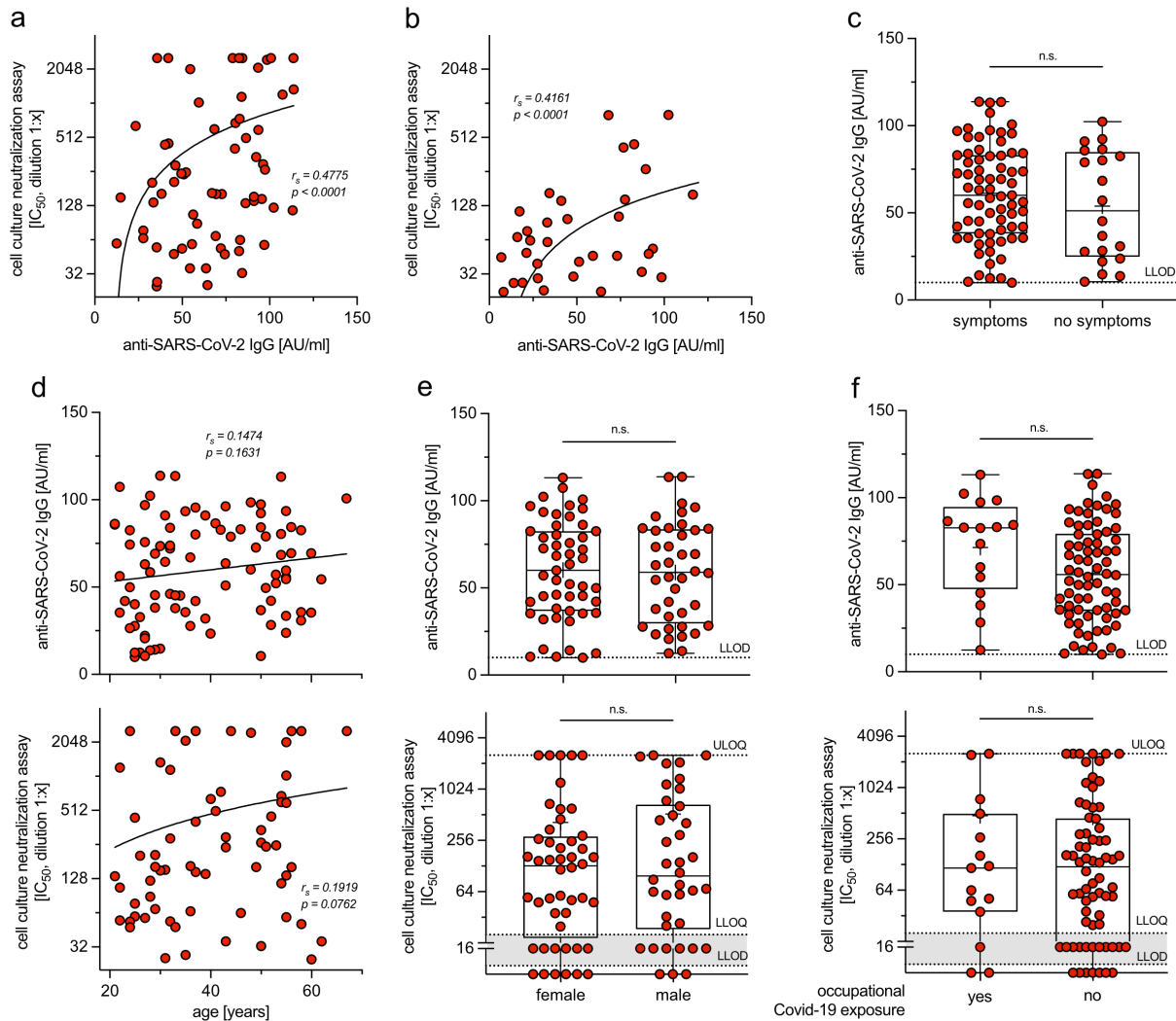


**d**

	convalescent individuals n = 91	naïve individuals n = 53
<b>sex</b>		
male	40 (44.0 %)	20 (37.7 %)
female	51 (56.0 %)	33 (62.3 %)
<b>mean age <math>\pm</math> SD</b>	39 $\pm$ 13 years	42 $\pm$ 20 years
<b>field of work</b>		
physician	15 (16.5 %)	6 (11.3 %)
nursing	18 (19.8 %)	11 (20.8 %)
medical assistance	5 (5.5 %)	2 (3.8 %)
research / laboratory	10 (11.0 %)	11 (20.8 %)
IT	10 (11.0 %)	5 (9.4 %)
administration	7 (7.7 %)	8 (15.1 %)
student	16 (17.6 %)	7 (13.2 %)
other	10 (11.0 %)	6 (11.3 %)
<b>patient contact</b>	49 (53.8 %)	27 (50.9 %)
<b>COVID-19 patient contact</b>	16 (17.6 %)	14 (26.4 %)
<b>risk factors</b>		
smoking	7 (7.7 %)	11 (20.8 %)
<b>pre-existing conditions</b>	19 (20.9 %)	17 (32.1 %)
respiratory conditions	7 (7.7 %)	3 (5.7 %)
cardiovascular conditions	4 (4.4 %)	4 (7.5 %)
diabetes mellitus	5 (5.5 %)	0 (0.0 %)
immune deficiency	0 (0.0 %)	1 (1.9 %)
immune suppression	0 (0.0 %)	2 (3.8 %)
other	4 (4.4 %)	8 (15.1 %)
<b>symptoms</b>	71 (78.0 %)	18 (34.0 %)
fever	49 (53.8 %)	5 (9.4 %)
coughing	46 (50.5 %)	6 (11.3 %)
dyspnea	21 (23.1 %)	4 (7.5 %)
cold symptoms	67 (73.6 %)	14 (26.4 %)
loss of smell / taste	45 (49.4 %)	4 (7.5 %)
fatigue / exhaustion	62 (68.1 %)	13 (24.5 %)
headache	45 (49.4 %)	8 (15.1 %)
diarrhea	19 (20.9 %)	3 (5.7 %)

Supplementary Figure 1 | Characteristics of anti-SARS-CoV-2 IgG seropositive study participants

(a) time axis of long-term follow-up in SARS-CoV-2 convalescents. (b) overview of the prospective study. (c) individual characteristics of study participants with  $\geq 2$  positive anti-SARS-CoV-2 IgG assays and reports on symptoms during SARS-CoV-2 infection. (d) characteristics of the study cohort for the seroprevalence testing.



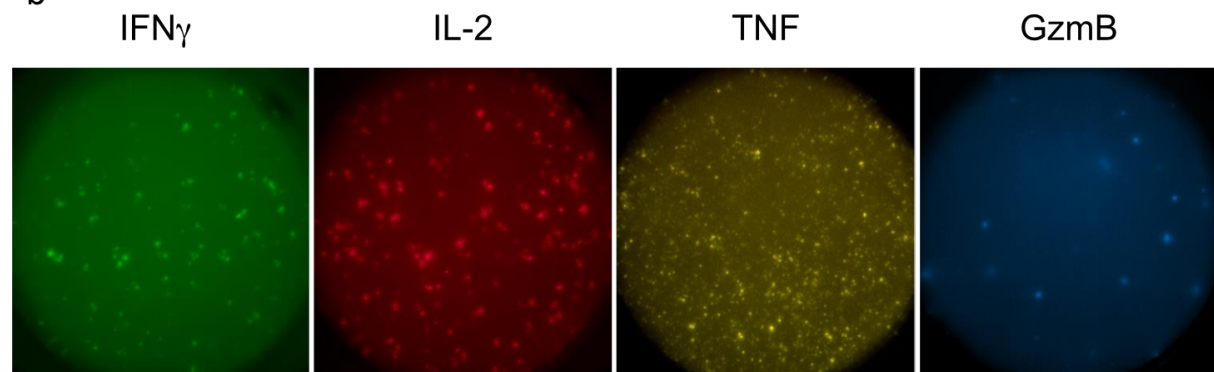
Supplementary Figure 2 | Characteristics of the dynamics of anti-SARS-CoV-2 IgG levels and virus-neutralization activities in convalescent individuals

(a,b) correlation of anti-SARS-CoV-2 IgG levels with virus-neutralization activity of convalescents at month 2 (a) and month 5 (b) after SARS-CoV-2 infection, 21 samples (a) or 57 samples (b) were below the quantification limit and are not shown but were included in the statistical analysis. (c) reporting of symptoms ( $n=71$ ) or no symptoms ( $n=20$ ) in convalescents and anti-SARS-CoV-2 IgG levels. LLOD – lower limit of detection. Data is shown, respectively, as median (60.13 and 51.18) with box bounds at 25% (38.15 and 24.74) and 75% percentile (83.09 and 84.95), whiskers show maxima (113.8 and 102.3) and minima (10.01 and 10.52). (d) correlation of anti-SARS-CoV-2 IgG levels and virus-neutralization activity with age of convalescents. 21 samples were below the quantification limit and are not shown (lower row). (e,f) anti-SARS-CoV-2 IgG levels and virus-neutralization activity in convalescents according to sex ( $n=51$ ,  $n=48$  (female);  $n=40$ ,  $n=38$  (male), respectively) or occupational exposure to COVID-19 patients ( $n=16$ ,  $n=15$  (yes);  $n=74$ ,  $n=70$  (no), respectively). LLOQ – lower limit of quantification; ULOQ – upper limit of quantification. Data is shown, respectively, as median (f: 60.13, 129.00 and m: 59.01, 97.75; yes: 82.73, 116.6 and no: 55.93, 120.8) with box bounds at 25% (f: 36.74, 18.23 and m: 29.61, 23.13; yes: 47.55, 35.80 and no: 34.91, 16.00) and 75% percentile (f: 82.56, 284.00 and m: 83.75, 672.70; yes: 94.71, 505.7 and no: 79.33, 444.8), whiskers show maxima (f: 113.2, 2560 and m: 113.8, 2560; yes: 113.2, 2560 and no: 113.8, 2560) and minima (f: 10.01, 1.0 and m: 12.51, 1.0; yes: 12.45, 1.0 and no: 10.01, 1.0). Statistical analyses by two-sided Mann-Whitney (c,e,f), and by Spearman correlation (a,b,d);  $r_s$  denotes Spearman correlation coefficient; n.s. denotes not significant.

a

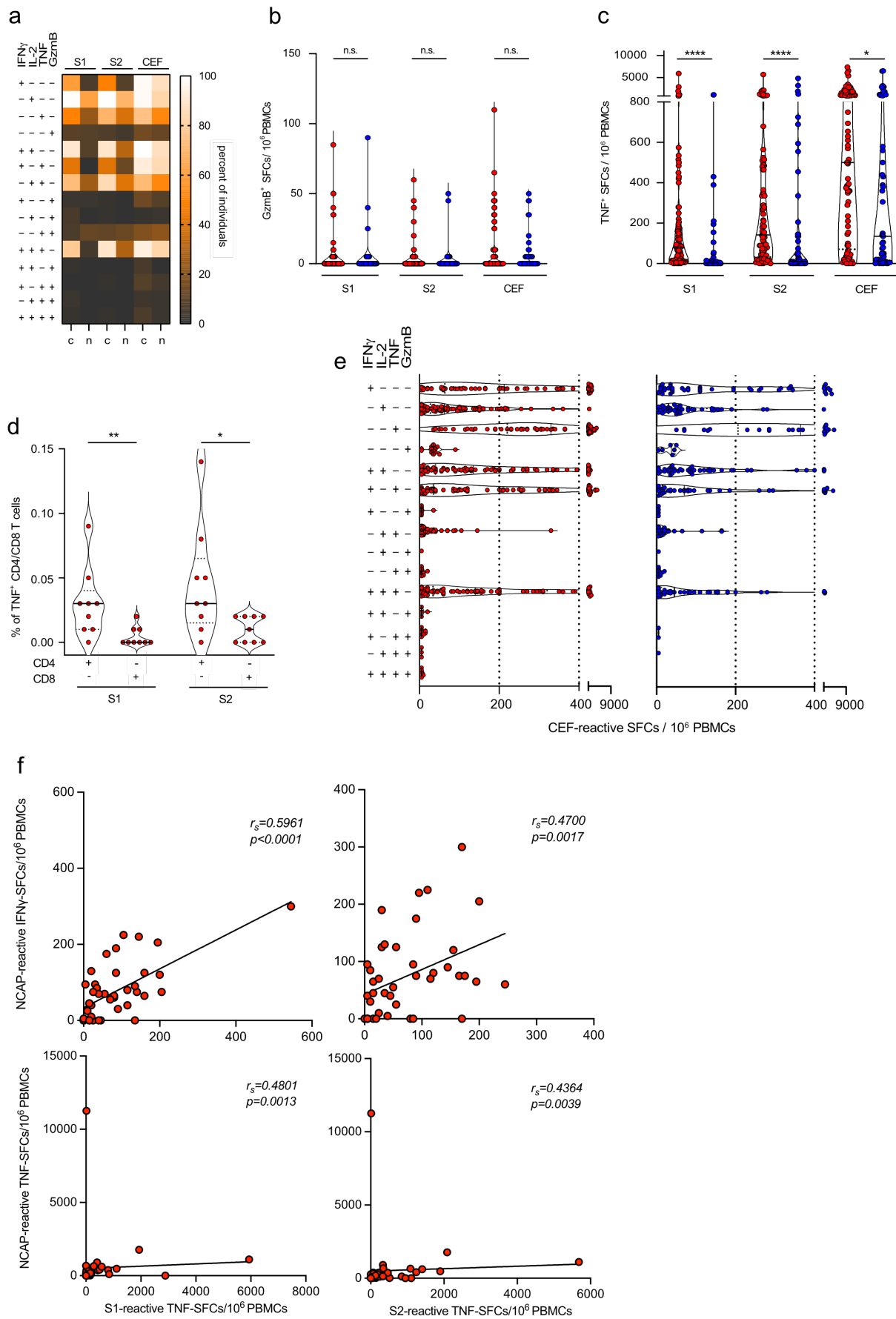
	CV (%)			
Parameter	IFN $\gamma$	IL-2	TNF	GzmB
Intra-assay variation (well to well; 4 replicates)	4.9	6.6	5.5	13.6
Inter-assay variation (plate to plate)	3.1	2.7	5.0	8.1
Inter-assay variation (day to day)	5.5	8.4	8.4	10.8
Inter-operator	6.6	11.1	4.8	6.7

b



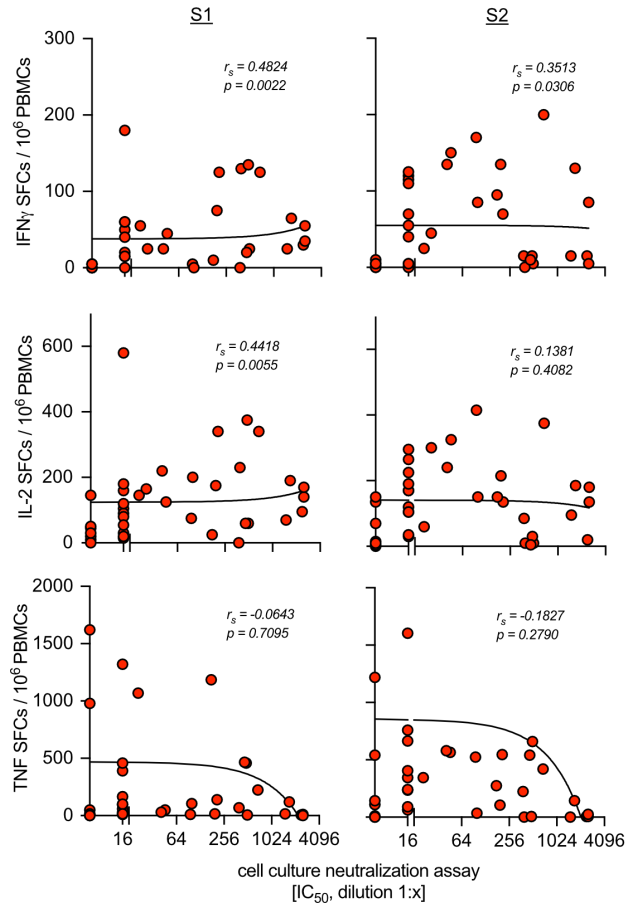
Supplementary Figure 3 | Performance of the four-color Fluorospot assay to detect spike-reactive cytokine-secreting cells directly *ex vivo* in  $10^6$  peripheral blood mononuclear cells (PBMCs)

(a) report of the Fluorospot assay characteristics. (b) representative images of the Fluorospot assay detecting frequencies of cytokine secreting cells among  $10^6$  PBMCs from a convalescent individual stimulated with the S1-peptide pool.



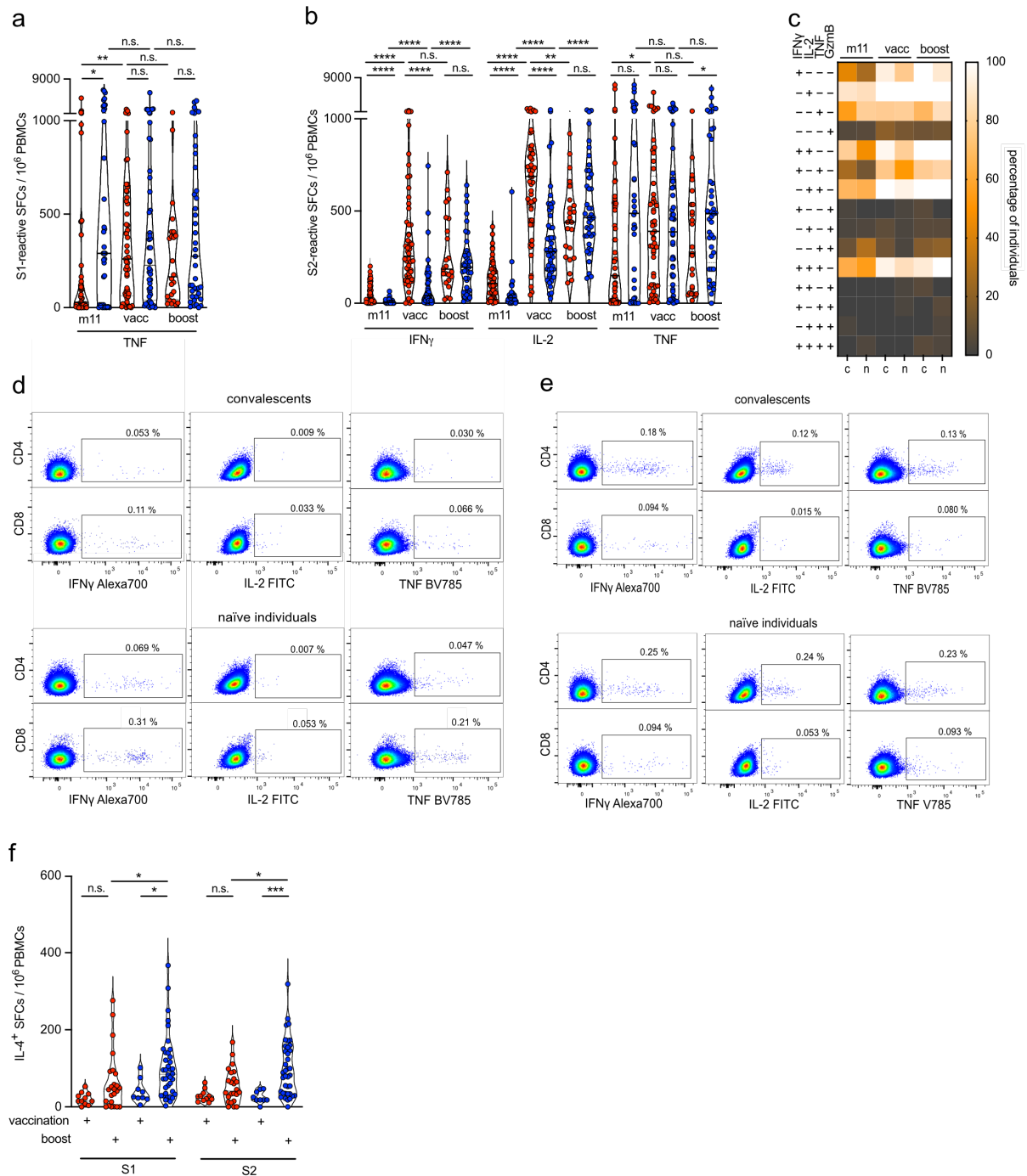
Supplementary Figure 4 | Characteristics of spike-reactive and CEF-reactive cytokine-secreting cells in convalescents and naïve individuals

(a) heatmap of individuals with mono- or polyfunctional S1-/S2-/CEF-reactive cytokine-secreting cells in convalescents (c) and naïve individuals (n) by direct *ex vivo* Fluorospot analysis at month 5 after SARS-CoV-2 infection. (b) frequencies of S1-/S2-/CEF-reactive GzmB-secreting cells; convalescents (red, n = 88), naïve individuals (blue, n = 52). (c) S1-/S2-/CEF-reactive TNF-secreting cells by direct *ex vivo* Fluorospot analysis; convalescents (red, n = 88), naïve individuals (blue, n = 52). (d) frequencies of S1- or S2-reactive TNF-secreting CD4 or CD8 T cells in convalescents (red, n = 9) determined by direct *ex vivo* intracellular cytokine staining and flow cytometric detection. (e) frequencies of mono- and poly-functional CEF-reactive cytokine-secreting cells by direct *ex vivo* Fluorospot analysis. (f) correlation of the frequencies of nucleocapsid- (NCAP) and S1- and S2-reactive T cells determined by Fluorospot analysis in convalescents at month 5; convalescents (red), naïve individuals (blue). Statistical analyses by two-sided Mann-Whitney, two-sided Wilcoxon signed-rank tests and by Spearman correlation and linear regression (b,c,d,f); rs denotes Spearman correlation coefficient; n.s. denotes not significant; \*p<0.05; \*\*p<0.01; \*\*\*\*p< 0.0001.



Supplementary Figure 5 | Correlation of spike-reactive cells with spike-specific antibodies and neutralization activity and dynamics of spike- and CEF-reactive cytokine-secreting cells over time

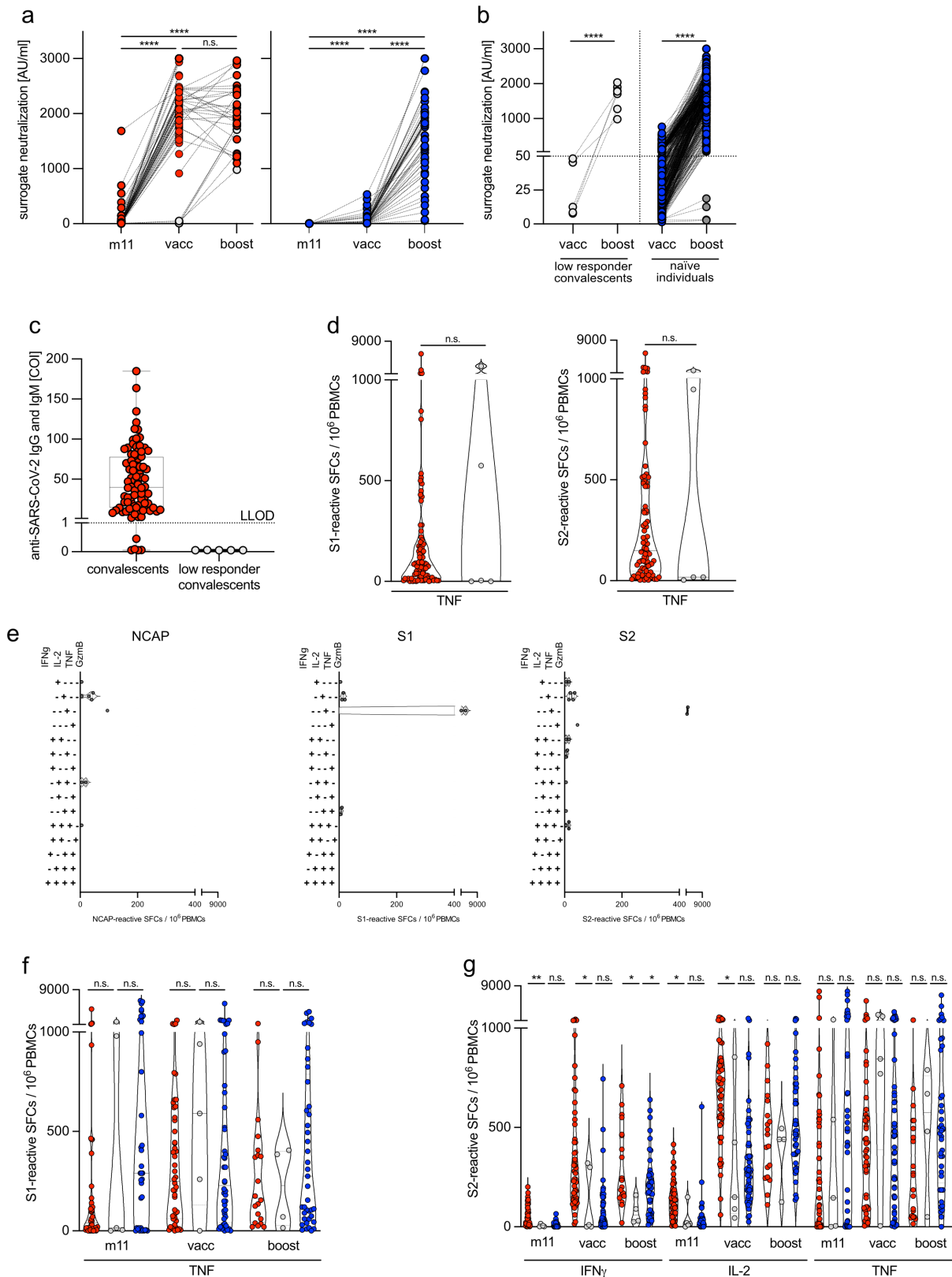
Spearman correlation of S1- and S2-reactive cytokine-secreting cells from convalescents with cell culture virus-neutralization activity of serum at month 11 after SARS-CoV-2 infection.  $r_s$  denotes Spearman correlation coefficient.



Supplementary Figure 6 | Frequencies of spike-reactive cytokine-secreting cells at month 11 after SARS-CoV-2 infection or after BNT162b2 mRNA prime and boost vaccination

(a,b) frequencies of spike-reactive cytokine-secreting cells determined directly *ex vivo* by Fluorospot analysis at month 11 after SARS-CoV-2 infection, at 2 weeks after BNT162b2 mRNA prime vaccination (vacc) or at 2 weeks after boost vaccination (boost); convalescents (red, n=50 (m11), n=54 (vacc), n=23 (boost)), naïve individuals (blue, n = 39 (m11), n = 49 (vacc), n = 40 (boost)). (c) heatmap of frequencies of individuals bearing spike-reactive cytokine-secreting cells, c - convalescents, n - naïve individual. (d,e) intracellular cytokine staining of spike-reactive CD4 and CD8 T cells determined directly *ex vivo* by flow cytometry, time points as in (a). (f) frequencies of spike-reactive IL-4-secreting cells after BNT162b2 mRNA prime vaccination (vacc) or boost vaccination (boost); convalescents (red, n = 11 (vacc), n = 24 (boost)), naïve individuals (blue, n = 9 (vacc), n = 38 (boost)). Statistical analyses by ANOVA, two-sided Mann-Whitney and two-sided Wilcoxon signed-rank tests (a, b, f); n.s. denotes not significant, \*p<0.05; \*\*p<0.01; \*\*\*p<0.001; \*\*\*\*p<0.0001.

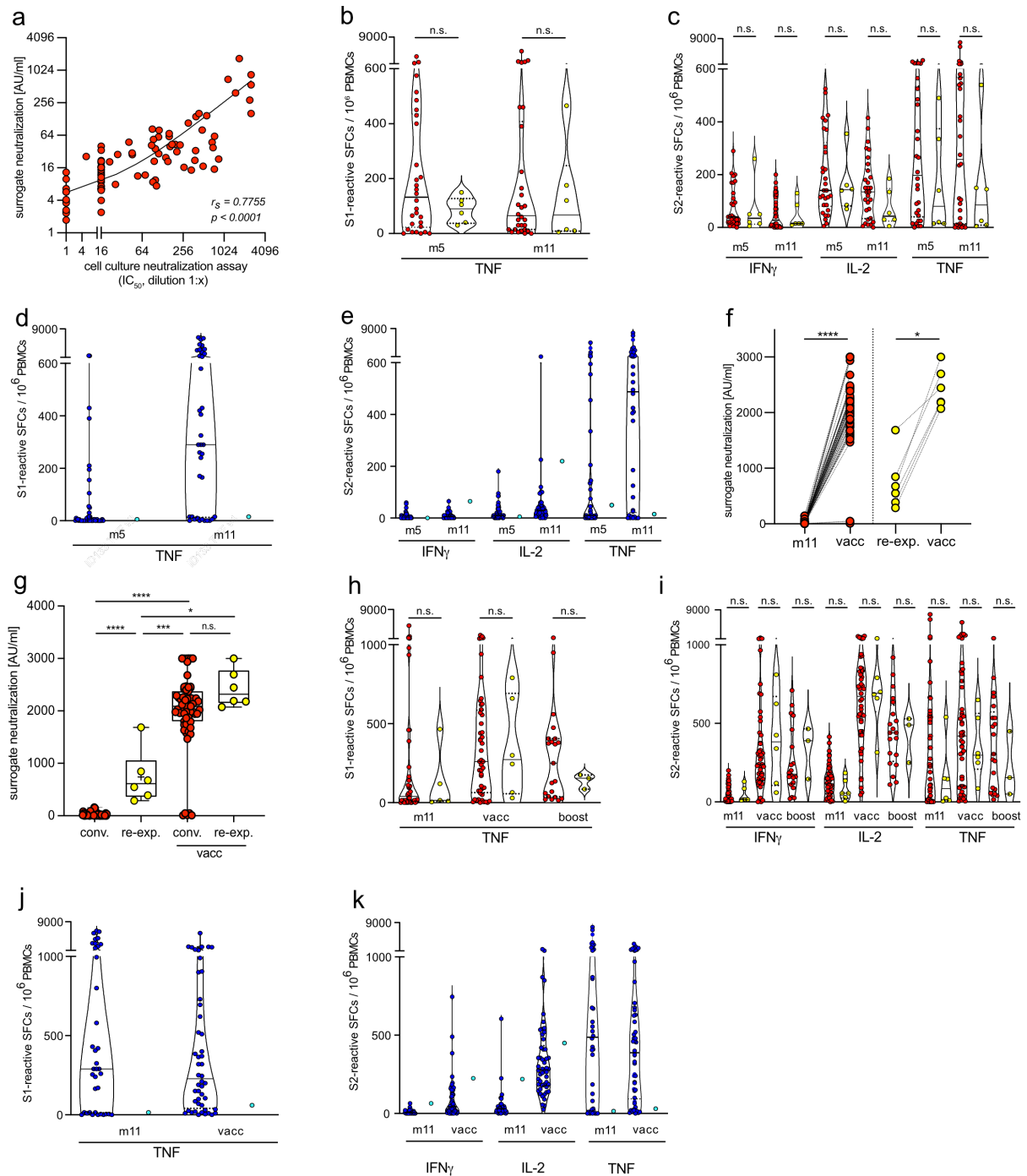




Supplementary Figure 7 | Lack of spike-specific immunity in convalescents with a delayed response to BNT162b2 mRNA vaccination

(a) individual courses of surrogate virus-neutralization activity in convalescents (red,  $n = 59$  (m11),  $n = 82$  (vacc),  $n = 33$  (boost)) after prime and boost BNT162b2 mRNA vaccination compared to naïve individuals (blue,  $n = 36$  (m11),  $n = 51$  (vacc),  $n = 49$  (boost)). (b) individual courses of surrogate virus-neutralization activity in a separate cohort of naïve individuals ( $n = 455$ ) after prime and boost BNT162b2 mRNA vaccination (right panel) demonstrating four individuals with a low response to vaccination (dark grey), compared to virus-neutralization

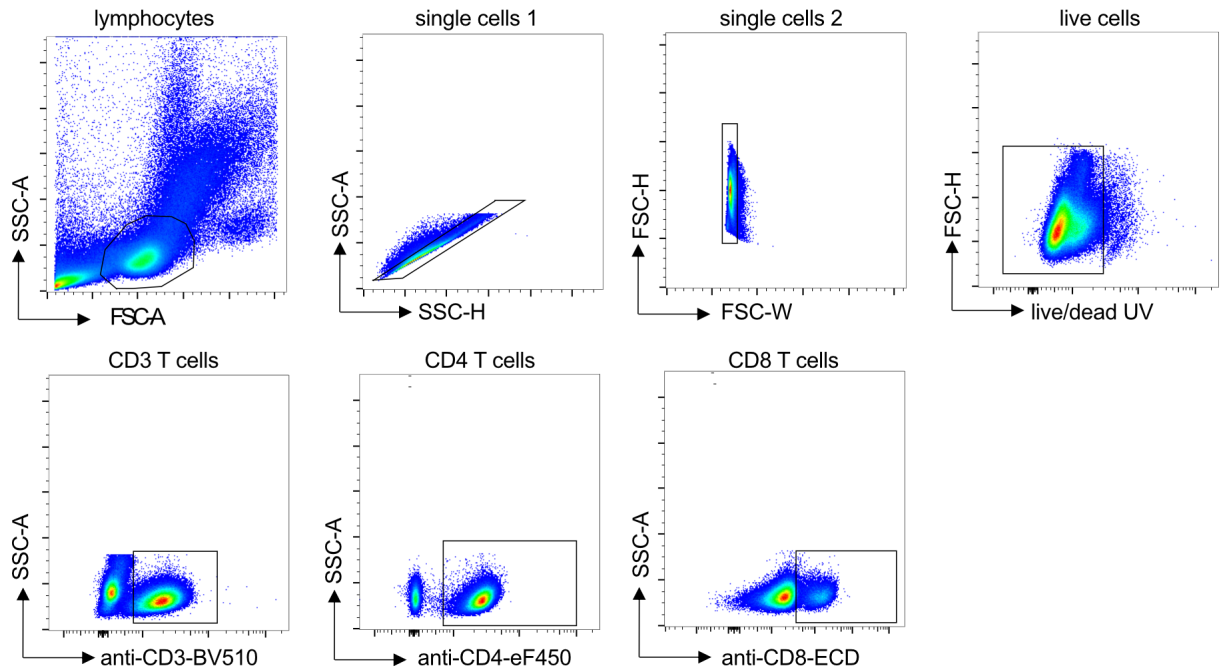
activity in low responder convalescents (n = 5) after vaccination (left panel). (c) anti-SARS-CoV2 IgG levels in low-level non-responder convalescents (grey, n = 5) compared to convalescents (red, n = 86) at month 2. (d) spike-reactive TNF-secreting cells at month 5 after infection in convalescents (red, n = 83) and convalescents with low response to vaccination (grey, n = 5). (e) fluorospot analysis revealing the frequencies of spike-reactive and nucleocapsid-reactive mono- and polyfunctional cytokine-secreting cells (spot-forming cells/SFCs in  $10^6$  PBMCs from low responder convalescents at month 5 after SARS-CoV-2 infection. (f,g) frequencies of spike-reactive cytokine-secreting cells at month 11 after SARS-CoV-2 infection, two weeks after prime (vacc) and two weeks after boost vaccination (boost) in convalescents (red, n = 45 (m11), n = 49 (vacc), n = 19 (boost)), convalescents with low response to vaccination (grey, n = 5 at all time points) and naive individuals (blue, n = 39 (m11), n = 49 (vacc), n=40 (boost)). Statistical analyses by ANOVA, two-sided Mann-Whitney and two-sided Wilcoxon signed-rank tests (a,b,c,d,f,g); n.s. denotes not significant; \* p<0.05; \*\* p<0.01; \*\*\*\* p< 0.0001



Supplementary Figure 8 | Characteristics of spike-specific immunity in convalescents compared to an individual after SARS-CoV-2 infection

(a) correlation between cell culture neutralization assay (shown as dilution 1:x mediating a 50% inhibition of SARS-CoV-2 infection *in vitro* - IC<sub>50</sub>) with a competitive CLIA (YHLO) measuring surrogate neutralization (arbitrary units (AU)/ml) at month 5 after SARS-CoV-2 infection. (b,c) frequencies of S1- or S2-reactive cytokine-secreting cells in convalescents (red, n = 32 (m5), n = 30 (m11)) or convalescents with increased virus-neutralizing activity (yellow, n = 6) at month 5 and month 11 after SARS-CoV-2 infection. (d,e) frequencies of S1- or S2-reactive cytokine-secreting cells in naïve individuals (blue, n = 51 (m5), n=39 (m11)) or the infected individual (turquoise, n = 1) at month 5 and month 11 after SARS-CoV-2 infection. (f) individual analysis of surrogate neutralization activity before and after BNT162b2 mRNA vaccination in convalescents (red, n = 60 (m11), n = 63 (vacc)) or convalescents with increased virus-neutralizing activity (yellow, n = 6). (g) surrogate neutralization activity in convalescents (red, n = 60 (m11), n = 63 (vacc)) and convalescents with increased virus-neutralizing activity (yellow, n = 6) before and after BNT162b2 mRNA vaccination. Data is shown, respectively, as median

(m11: 16.81, 613.2 and vacc: 2087, 2319) with box bounds at 25% (m11: 7.275, 363.10 and vacc: 1801, 2153) and 75% percentile (m11: 33.15, 1055 and vacc: 2376, 2772), whiskers show maxima (m11: 161.9, 1684 and vacc: both 3000) and minima (m11: 1.73, 286.5 and vacc: 7.73, 2072). (h,i) frequencies of S1 or S2-reactive cytokine-secreting cells in convalescents (red, n = 44 (month 11), n = 48 (vacc), n = 20 (boost)) or convalescents with increased virus-neutralizing activity (yellow, n = 6) before vaccination (month 11), 2 weeks after vaccination (vacc) and 2 weeks after boost vaccination (boost). (j,k) frequencies of S1- or S2-reactive cytokine-secreting cells in naïve individuals (blue, n = 39 (month 11), n = 49 (vacc), n = 40 (boost)) or the infected individual (turquoise, n = 1) before vaccination (month 11) and 2 weeks after vaccination (vacc). Statistical analyses by ANOVA, two-sided Mann-Whitney, two-sided Wilcoxon signed-rank tests (b,c,f,g,h) and by Spearman correlation (a) and linear regression.  $r_s$  denotes Spearman correlation coefficient; n.s. denotes not significant \* $p < 0.05$ ; \*\*\* $p < 0.001$ ; \*\*\*\* $p < 0.0001$



Supplementary Figure 9 | Gating strategy for flow cytometry.

Peripheral blood lymphocytes were gated based on size, single cells, live/dead staining, staining with anti-CD3 to identify T cells. Subsequent differentiation of T cell populations was based on CD4 and CD8 surface staining.

**Data availability:** All data generated in this study are provided in the Supplementary Information/Source Data Files. The study protocols for the SeCoMRI and VaCoMRI studies are available upon request.